Geomechanics and Engineering, *Vol. 41, No. 1 (2025) 1-10*
https://doi.org/10.12989/gae.2025.41.1.001

Sustainable soil stabilization using calcium sulfoaluminate cement and phosphogypsum

Anna Loskutova[a], Jong Kim[b], Alfrendo Satyanaga[c], Sung-Woo Moon*

Department of Civil and Environmental Engineering, School of Engineering and Digital Sciences
Nazarbayev University, 53, Kabanbay bater Ave., Astana, 010000, Republic of Kazakhstan

(*Received December 4, 2024, Revised March 4, 2025, Accepted March 5, 2025*)

Abstract. Various additives, including fly ash, lime, fibers, and slag, have been extensively examined to improve soil stabilization properties and achieve targeted performance standards. Among these, Calcium Sulfoaluminate (CSA) cement has garnered significant attention for its environmentally friendly profile as compared to ordinary Portland cement (OPC), alongside its rapid strength development and high durability. This study investigates the effects of substituting CSA with phosphogypsum (PG) to enhance the compressive strength of sand while addressing the recycling potential of waste produced from phosphorus manufacturing. The chemical composition of PG was analyzed using X-ray fluorescence (XRF) and X-ray diffraction (XRD), revealing calcium sulfate hemihydrate as the primary component, along with impurities such as fluorine, phosphorus, silicon, and sulfur compounds. Standardized mixture compositions containing 3%, 5% and 7% CSA and 10% water were prepared, with CSA partially replaced by PG at substitution rates of 10%, 20%, 30%, 40%, and 50%. Uniaxial compressive strength (UCS) and ultrasonic pulse velocity (UPV) tests were performed at curing intervals of 3, 7, 14, and 28 days to evaluate the influence of PG on soil stabilization properties. Additionally, scanning electron microscopy was used to analyze the microstructural changes underlying the observed strength gain. The results demonstrate that substituting 30% of CSA with PG yields the highest compressive strength after 28 days of curing, indicating the optimal replacement level. These findings highlight the dual benefits of improved soil stabilization performance and sustainable recycling of industrial byproducts, offering practical implications for eco-friendly construction and waste management practices.

Keywords: compressive strength; CSA-treated sand; phosphogypsum; soil stabilization; sustainability

1. Introduction

Soil stabilization is a critical activity in civil engineering, especially in regions with soft, friable, or otherwise unsuitable soils lack the necessary strength and stability to support large structures without modification (Gidebo *et al.* 2023, Javad Jalili 2023). Traditionally, the construction sector has relied on Portland cement or lime to stabilize soil properties such as load-bearing capacity and durability (Akın Altun and Sert 2004, Ahmadullah and Chrysochoou 2024, Regasa *et al.* 2023, Subramanian *et al.* 2024, Zivari *et al.* 2023). However, these conventional methods have significant environmental and economic drawbacks (Jain, 2024, Mustafayeva *et al.* 2023a, Mustafayeva *et al.* 2023b, Ocheme *et al.* 2023, Sagidullina *et al.* 2022a). For example, Portland cement production is associated with high carbon emissions, making a major contributor to global climate change.

In response to these challenges, calcium sulfoaluminate (CSA) cement has emerged as a promising alternative due to its lower carbon footprint and rapid early strength development (Sagidullina *et al.* 2023, Sagidullina *et al.* 2022b, Subramanian *et al.* 2024). These properties make CSA cement particularly advantageous for projects requiring accelerated construction timelines or rapid stabilization (Sagidullina *et al.* 2022, Subramanian *et al.* 2019). Beyond traditional binders, industrial by-products have also gained attention for their cost effectiveness and environmental benefits in soil stabilization (Kayumov *et al.* 2021, Murali and Azab 2023, Qin *et al.* 2023).

Phosphogypsum (PG), a by-product of phosphoric acid production, is one such material with considerable potential in the sustainable construction industry (Men *et al.* 2022, Meskini *et al.* 2023). Generated in large quantities, PG primarily consists of calcium sulfate, which plays a critical role in cement hydration and can enhance the strength and durability of stabilized soils (Degirmenci *et al.* 2007). Properly processed PG can serve as sustainable supplement or partial replacement for conventional binders in soil stabilization, while simultaneously addressing the environmental challenge of PG waste management.

The combination of CSA cement and PG offers significant benefits, potentially yielding a cost-effective, and environmentally friendly soil stabilizer. The calcium sulfate in PG interacts with CSA cement to promote the formation of ettringite, gel phases, and other compounds that enhance soil cohesion and bonding. This synergy can improve the compressive strength of treated soils, reduce

*Corresponding author, Associate Professor
E-mail: sung.moon@nu.edu.kz
[a]Graduate Student
[b]Professor
[c]Associate Professor

ISSN: 2005-307X (Print), 2092-6219 (Online)

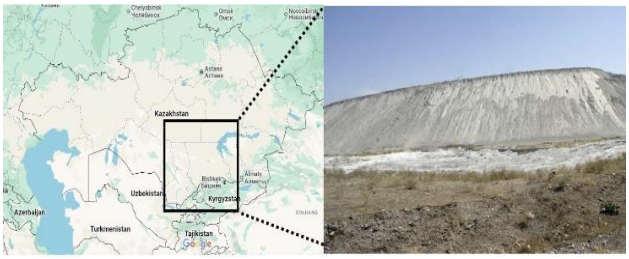

Fig. 1 Location of Phosphogypsum; Taraz, Kazakhstan

reliance on traditional materials, and mitigate the environmental impact of phosphoric acid industry (Aparna and Bindu 2023, Degirmenci *et al.* 2007).

Although the use of phosphogypsum as a building material has been studied previously, other studies have mainly focused on its use with Portland cement and have not been successful because phosphogypsum contained large amounts of impurities. Also, the combination of phosphogypsum with CSA has not been studied. Although these studies demonstrate the potential of PG to improve material properties, they often ignore important aspects such as the effect of different PG proportions, optimization of PG-CSA ratios, and the evolution of microstructural changes over time.

This study investigates the mechanical and microstructural effects of incorporating PG into CSA-treated sand. Specifically, the study examines the effect of varying PG proportions on the compressive strength of CSA-treated sand, the optimum CSA and PG ratios that maximize strength, changes in material performance over different curing periods to understand how the PG-CSA combination behaves over time, and the microstructure of the resulting materials.

Fig. 1 shows the location of PG source in Taraz, Kazakhstan, where the material was obtained from the "KazPhosphat" industrial facility (see Fig. 1). The region is a major center for phosphate mining and processing, resulting in substantial PG stockpiles. These stockpiles, often stored in open areas, pose significant environmental concerns (Wu *et al.*2022, Zheng *et al.*2023). By leveraging PG in soil stabilization, this study addresses both geotechnical challenges and environmental sustainability, making it particularly relevant for regions like Kazakhstan, where poor soil conditions and the widespread availability of industrial by-products create a strong need for sustainable stabilization solutions.

2. Experimental procedure

This study investigates the effect of different ratios of PG and CSA cement on the compressive strength and microstructure of treated sand. The procedure encompasses several stages: preparation and analysis of raw materials, mixing of samples with varying proportions, curing under controlled conditions, and conducting mechanical and microstructural tests.

2.1 Materials

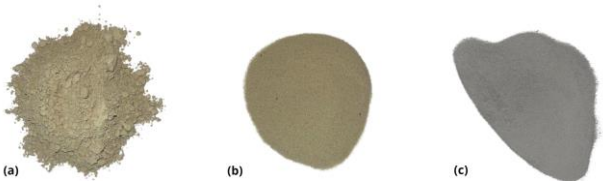

Fig. 2 Materials: (a) CSA, (b) Sand, and (c) PG

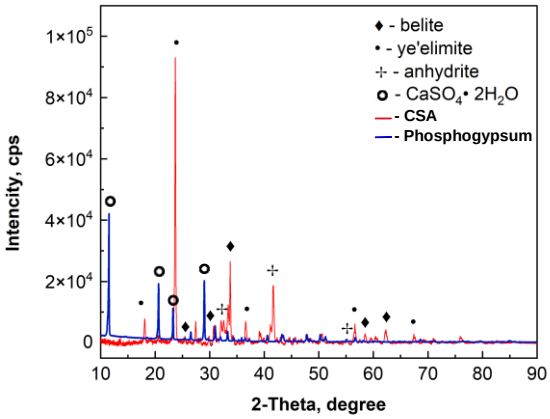

Fig. 3 XRD analysis of PG and CSA

The primary materials used in this study are CSA cement, quartz sand, and PG.

CSA cement was chosen for its rapid strength development and low carbon footprint compared to Portland cement (Subramanian *et al*. 2019).

CSA cement, composed primarily of ye'elimite and belite, enhances both early and long-term strength as well as durability. It is a fine, light brown powder (see Fig. 2(a)) and is stored in sealed packaging to prevent pre-hydration, ensuring tis optimal performance in cementitious applications.

Fine, clean and dry brown sand with uniform particle size distribution served as the base material for the test specimens (see Fig. 2(b)). According to the Unified Soil Classification System (USCS), the sand is classified as poorly graded sand. The sand was dried at 100°C to remove residual moisture that could interfere with the curing process and test results.

PG was collected from a local phosphoric acid plant and prepared by drying and sieving. Since raw PG tends to form lumps, sieving produced a fine powder, ensuring uniform mixing and enhancing reactivity with CSA cement (Rashad 2017). After sieving, the material exhibited a consistency similar to other mixing materials components and had a light grey color.

To ensure suitability of PG for soil stabilization, its chemical composition was analysed using X-ray diffraction (XRD). The analysis of CSA was also performed in this study.

High impurity levels in PG can negatively impact the environment (Liu *et al.* 2019, Saadaoui *et al.* 2017), necessitating this analysis. XRD analysis identified the mineral phases in PG, confirming its high calcium sulfate

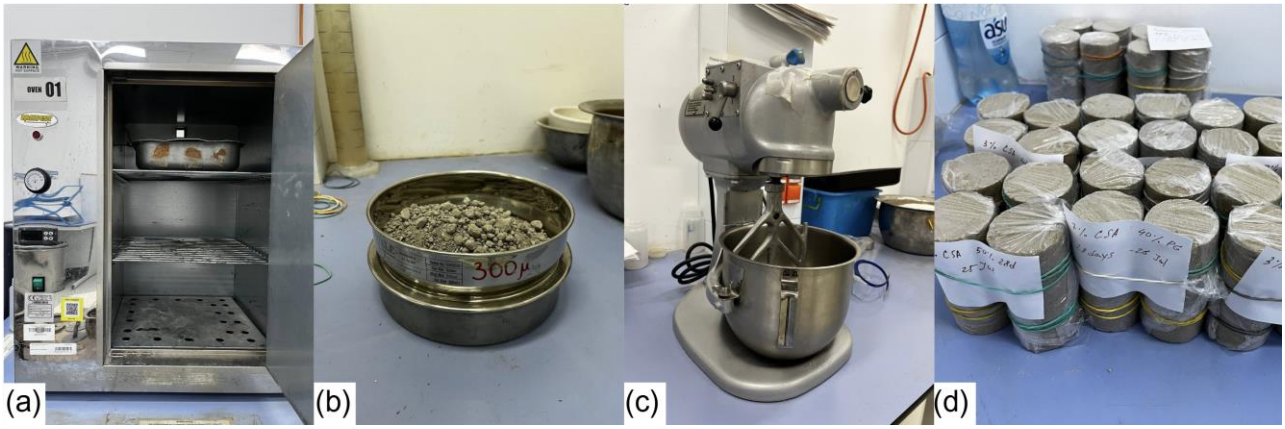

Fig. 4 Sample Preparation Process:(a) Drying of sand and PG for 24 hours; (b) Sieving of PG; (c) Mixing of materials and (d) Curing for 3, 7, 14, and 28 days

Table 1 Proportions of materials for different PG replacement levels at CSA 7%

PG Replacement %	7% CSA (g)	PG (g)
10	85.6	9.6
20	76.2	19.0
30	66.6	28.6
40	57.1	38.1
50	47.6	47.6

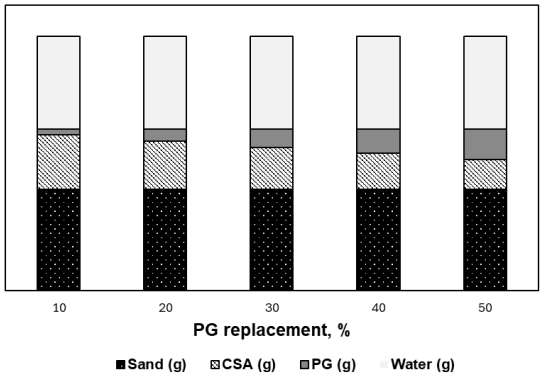

Fig. 5 Proportions of materials for different PG replacement levels

(gypsum) content (see Fig. 3) and detecting any secondary phases that could influence the stabilization process.

The CSA XRD results found three main phases, which are belite, ye'elimite and anhydrite. This analysis provided critical information on the crystalline structure of PG and CSA, which plays a key role in the hydration and binding properties of CSA-treated sand mixtures. The compatibility of PG with CSA cement, as indicated by XRD results, ensures optimal performance in improving the compressive strength of treated soils.

2.2 Sample preparation and mixture ratios

The primary objective of this study is to prepare specimens with different CSA and PG contents to identify the optimal mixture ratio for maximum compressive strength. To ensure consistency and reliability, each combination was mixed, molded, and cured under identical conditions. The sample preparation process depicted in Fig. 4, involved several crucial steps, following the methodology outlined by Ocheme James (2024).

The CSA content was set at three levels: 3%, 5% and 7% of the total sand weight. PG was incorporated as a partial replacement for CSA at increments of 10%, 20%, 30%, 40%, and 50%. These concentrations were selected to facilitate comparisons with existing study on CSA replacement with gypsum, aiming to explore the potential use of industrial waste materials in construction sector.

To ensure consistency and repeatability, the water content was maintained at 10% throughout the study. This experimental design enabled a comprehensive analysis of the impact of increasing PG content on the strength and durability of the mixtures. Table 1 illustrates the material proportions, illustrating the progressive reduction in CSA content as PG replaces it in 10% increments, while sand and water content remain constant across all mixtures. Additionally, Fig. 5 provides a visual representation to enhance understanding of the mixing process and material distribution.

Prior to mixing, sand and PG were oven-dried at 100°C for 24 hours to eliminate residual moisture, ensuring uniform conditions across all samples. The dried PG was then sieved through a 300-micron mesh to obtain a fine, consistent powder, promoting homogeneous mixing and optimal reaction efficiency in the stabilized sand matrix. Sand, PG, CSA, and water were then thoroughly combined using a mechanical mixer for 10 minutes to achieve a homogeneous mixture. The prepared mixtures were subsequently molded into cylindrical specimens with dimensions of 50 mm in diameter and 100 mm in height, ensuring uniformity for compression testing. For initial curing, the samples were wrapped in plastic film and kept in molds for dry curing at room temperature in the laboratory. The dry curing method was selected because, unlike OPC, CSA cement does not require prolonged wet curing to achieve strength development. This approach also reflects real-world conditions where large-scale wet curing is

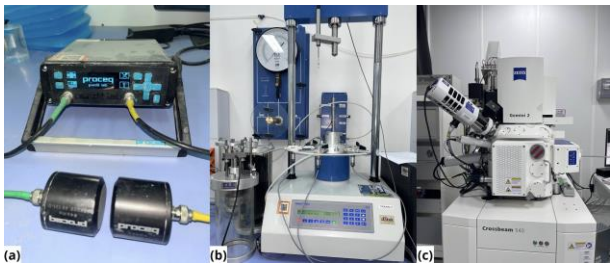

Fig. 6 Equipment used (a) UPV; (b) UCS and (c) SEM

impractical. After demolding, the specimens underwent final curing at 20°C for 3, 7, 14, and 28 days to evaluate strength development over time.

2.3 Testing methodology

The experimental process includes three main tests to analyze the strength development and microstructural changes. Fig. 6 shows the equipment used.

2.3.1 Ultrasonic pulse velocity test

The ultrasonic pulse velocity (UPV) test is a non-destructive method for assessing the internal structure and homogeneity of materials (Rauf *et al.* 2024). In this test, ultrasonic waves are transmitted through the specimen, and the time taken for the pulse to traverse the sample is measured (see Fig. 6(a)). Shorter travel times indicate higher density and better homogeneity (Sagidullina *et al.* 2023). The UPV results were compared with UCS values to evaluate the effectiveness of the PG-CSA combination in enhancing material quality.

2.3.2 Unconfined compressive strength test

The unconfined compressive strength (UCS) test measures the compressive strength of a material by determining the maximum axial load it can withstand (Rauf *et al*. 2024). In this study, specimens were subjected to a continuous axial load in a testing machine until failure (see Fig. 6(b)). The peak load at failure was recorded as the UCS value, representing the compressive strength of the mixture (Ocheme *et al*. 2024). The testing machine's parameters were calibrated using a computer application to ensure accurate data collection. To enhance the reliability of results, four specimens were tested for each composition, and the average UCS value was used for analysis.

2.3.3 Scanning electron microscopy

Scanning electron microscopy (SEM) was conducted to analyze the microstructure of PG-CSA-treated sand at a microscopic level (see Fig. 6(c)). This analysis provided insights into the distribution and bonding of particles, as well as the formation of hydration products such as ettringite, which plays a critical role in strength development (Guo *et al.* 2014).

Specimens were prepared for SEM by coating them with a thin layer of gold to enhance conductivity, ensuring high-resolution imaging and minimal distortion caused by electron accumulation. SEM images captured particle distribution, the bonding between CSA and PG, and the formation of hydration products. The analysis also revealed voids and porosity, offering valuable information on how different PG levels affect the microstructure and overall strength of the mixtures.

By systematically analyzing the results from UCS, UPV and SEM tests at various curing times and mix ratios, this methodology provides a comprehensive evaluation of the impact of PG on CSA-treated sand. These tests will identify the optimal PG-CSA combination for achieving maximum compressive strength and durability (Liu *et al*. 2019).

3. Results and discussion

3.1 UPV results

Fig. 7 illustrates the UPV results after 28 days of curing for different CSA concentrations (3%, 5%, and 7%) and varying PG replacement percentages (10%, 20%, 30%, 40%, and 50%). By analyzing the effect of CSA concentration and PG replacement levels using UPV, the optimal combination for improving material density and uniformity was determined.

At 3% CSA, UPV values are consistently lower across all PG replacement levels compared to higher CSA concentrations. At 10% PG replacement, the UPV reaches approximately 1300 m/s after 28 days. The highest value at this concentration, nearly 1500 m/s, is observed at 30 % PG replacement. However, higher PG replacements (40% to 50%) result in a decline in UPV values, indicating reduced uniformity and compactness due to excessive PG content.

At 5% CSA, UPV values improve significantly compared to 3% CSA. At 30% PG replacement, the UPV reaches approximately 1800 m/s after 28 days, reflecting better integrity and compaction. However, UPV values drop at 40% and 50% PG replacement, with values of approximately 1600 m/s and 1400 m/s, respectively, suggesting a decline in uniformity at higher PG levels.

At 7% CSA, the UPV values are the highest among all CSA concentrations, indicating excellent compaction and uniformity. At 30% PG replacement, the UPV value reaches approximately 2300 m/s after 28 days, the highest among all samples. This result highlights that a high CSA concentration combined with 30% PG replacement produces a dense, highly compact material. Although higher PG replacements (40% to 50%) reduce UPV values, they remain relatively high compared to lower CSA concentrations, indicating that 7% CSA mitigates the adverse effects of higher PG content on compactness.

3.2 UCS results

Fig. 8 presents the UCS results over a curing period of 3, 7, 14, and 28 days for samples containing different CSA concentrations (3%, 5% and 7%) and PG replacement percentages (10% - 50%).

At a 3% CSA concentration, UCS values were the lowest among the tested specimens. The highest value for this concentration, approximately 800 kPa, was recorded for specimens with 30% PG replacement after 28 days of curing. However, a notable decline in strength was observed when PG content exceeded 30%, suggesting that while moderate PG incorporation enhances mechanical performance, excessive replacement may compromise matrix cohesion and overall structural integrity.

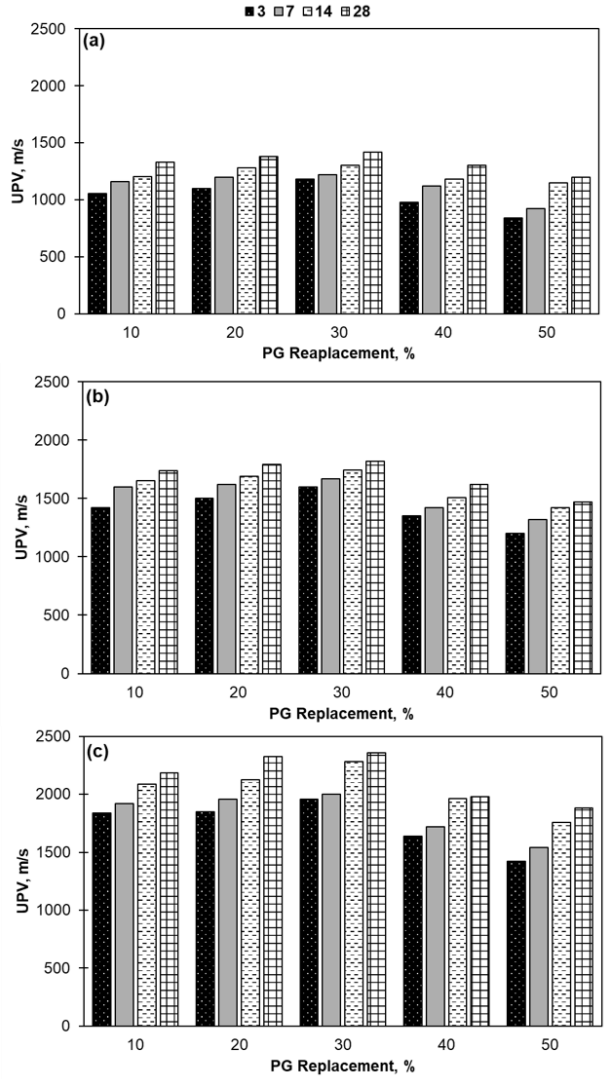

Fig. 7 Homogeneity of different PG replacements after 28 days of curing: (a) CSA 3%; (b) CSA 5% and (c) CSA 7%

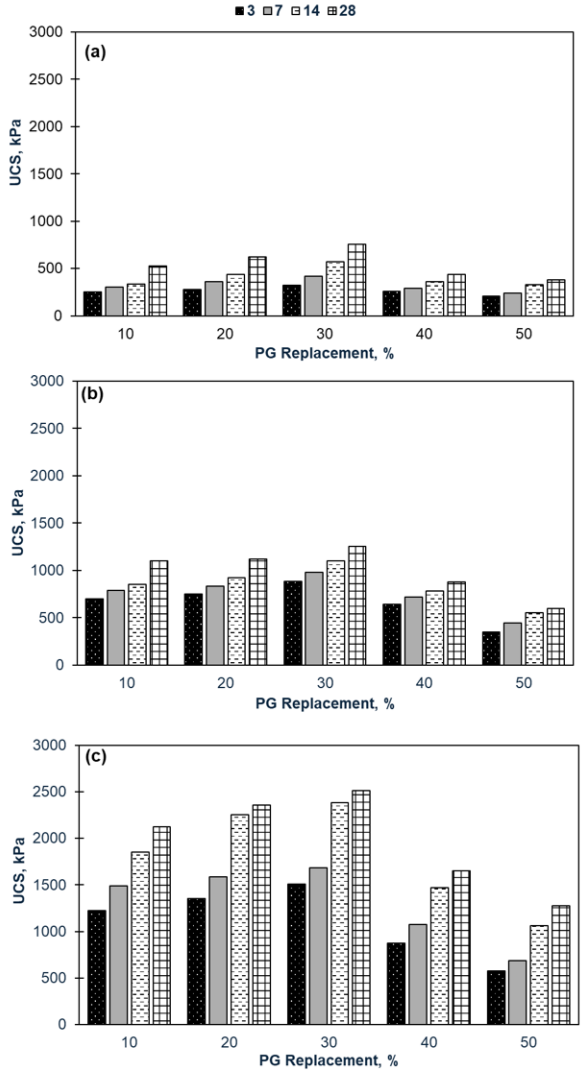

Fig. 8 Strength gain of different PG replacement % for 28 curing days: (a) CSA 3%; (b) CSA 5% and (c) CSA 7%

A notable trend observed across all CSA concentrations (3%, 5%, and 7%) is that the largest rate of strength gain occurs between 14 and 28 days, particularly for specimens with PG replacements ranging from 10% to 30%. Among these, the optimal concentration remains 30% PG replacement, which consistently yields the highest strength values.

Increasing the cement concentration from 3% to 5% nearly doubles the strength, while increasing to 7% results in fourfold increase. At 7% CSA with 30% PG replacement, the peak UCS value reaches 2500 kPa. The higher strength observed at 7% CSA is likely attributed to the increased sulfate content, which enhances hydration reactions and matrix bonding, leading to a more densified and well-structured microstructure. This trend aligns with previous findings (Rauf *et al*. 2024), further reinforcing the positive correlation between CSA content and strength development.

The results indicate that 7% CSA and 30% PG replacement combination achieves the optimal balance of strength and durability. Most hydration reactions occur within the first 28 days (Park *et al.* 2021, Tao *et al.* 2023). Similarly in this case significant strength gains observed between 14 and 28 days for 3% and 5% CSA concentrations, reflecting a difference of approximately 20%. However, for 7% CSA, the most notable strength increase occurs between 7 and 14 days, likely due to the optimized availability of hydration components, which accelerate the reaction process at an earlier stage. These findings underscore the importance of CSA dosage optimization in achieving superior mechanical performance in stabilized soils.

For comparison, reference data from previous studies on CSA-stabilized soil, including 0%, 30% and 50% gypsum replacement at an equivalent CSA content of 7% were examined. Notably, Subramanian *et al*. (2019) reported a maximum UCS of approximately 1400 kPa for 7% CSA with 0% gypsum replacement after 3 days of curing, followed by a progressive decrease in strength over longer curing periods. This trend suggests that the absence of gypsum in CSA-stabilized soils may lead to early strength gain due to rapid

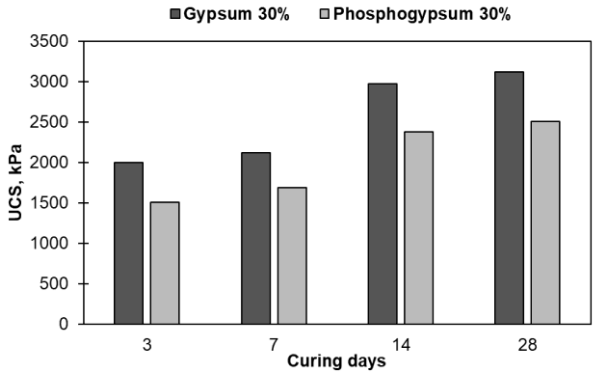

Fig. 9 Results with 30% gypsum and phosphogypsum content for 7% CSA-treated sand

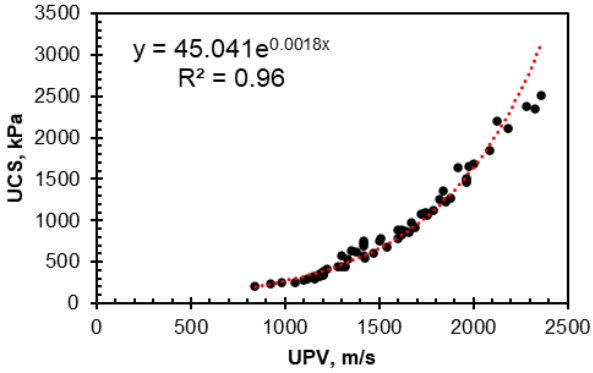

Fig. 10 The exponential relationship between UCS and UPV

hydration reactions, but subsequent reductions may result from microstructural changes, such as ettringite instability or delayed sulfate reactions. In contrast, the present study demonstrates that optimized PG incorporation (e.g., 30%) not only enhances early-age strength but also sustains long-term strength development, highlighting the beneficial role of PG in improving the durability and mechanical performance of CSA-stabilized soils, providing a sustainable alternative for soil stabilization in geotechnical applications.

3.2.1 Comparison of phoshogypsum and gypsum performance

The optimum content of PG was observed to be 30%. The following section will compare the performance of PG and gypsum with similar replacement proportion and CSA 7%. This test compares the performance of traditional gypsum with that of PG to assess its viability as an alternative.

Fig. 9 presents the UCS results over curing periods of 3, 7, 14 and 28 days for a sample containing the optimum gypsum (G) content in a CSA-treated sand mixture. The optimum gypsum content was determined to be 30%, as this proportion provided the best balance of compressive strength and material stability (Subramanian *et al*. 2019).

At the 3-day mark, the UCS reaches approximately 2000 kPa, demonstrating the rapid early strength development facilitated by CSA. After 7 days, the UCS increases further to approximately 2300 kPa, indicating continued hydration and matrix compaction. For PG the 7th day deviator peak stress was observed as 1800 kPa, which is lower than gypsum strength by approximately 20%. By the 28 days, the UCS has stabilized at around 3200 kPa, signifying the completion of most hydration reactions. Comparing to PG peak strength, the difference again was 20%.

This experiment emphasizes the importance of demonstrating that PG can serve as a viable alternative to traditional gypsum, which has a proven track record of improving compressive strength. While PG contains impurities that can affect the hydration process and results in slightly lower strength development, it still shows potential effectiveness.

3.2.2 Relationship between UPV and UCS

Fig. 10 illustrates the exponential relationship between UPV and UCS for CSA-treated sand with phosphogypsum replacement. The derived equation demonstrates a strong correlation, confirming UPV as a reliable predictor of UCS.

At low UPV values (<1500 m/s), UCS remains below 1000 kPa, reflecting early curing stages with limited hydration products. As UPV increases (1000–2000 m/s), UCS rises steadily due to material densification, CSH and ettringite's progressive formation. At high UPV values (>2000 m/s), UCS exceeds 1500 kPa, indicating the development of a well-structured matrix with strong bonding and enhanced mechanical integrity. This relationship validates the use of UPV as a non-destructive testing method to estimate UCS, making it an efficient tool for quality control and optimization in construction applications involving CSA and PG-treated sands.

This study establishes an exponential relationship between UCS and UPV with a strong correlation coefficient ($R^2 = 0.96$). Comparison with previous studies (Almeshal *et al*. 2020, Vinoth *et al.* 2018) further validate the reliability of UPV as a non-destructive predictor of UCS, although differences exist in UPV and UCS ranges.

The results indicate UCS values up to 3200 kPa at UPV values up to 2500 m/s, while the previous studies may extend to higher strengths. Variations in the exponential coefficient suggest differences in the rate of UCS development with increasing UPV, likely influenced by material composition, curing conditions, and stabilization methods. Despite these variations, the overall findings align with existing research, reinforcing the practical application of UPV for strength assessment in CSA-treated sand with PG replacement.

3.4 SEM results

Fig. 11 presents SEM images illustrating the microstructural evolution of CSA-treated sand with varying phosphogypsum (PG) replacement levels (10%, 30%, and 50%) after 7 days of curing. The images reveal the progressive formation of calcium silicate hydrate (CSH) gel and ettringite, along with the presence of pores and microcracks. To validate these observations, the findings were compared with previous studies on microstructural changes in CSA-enhanced materials

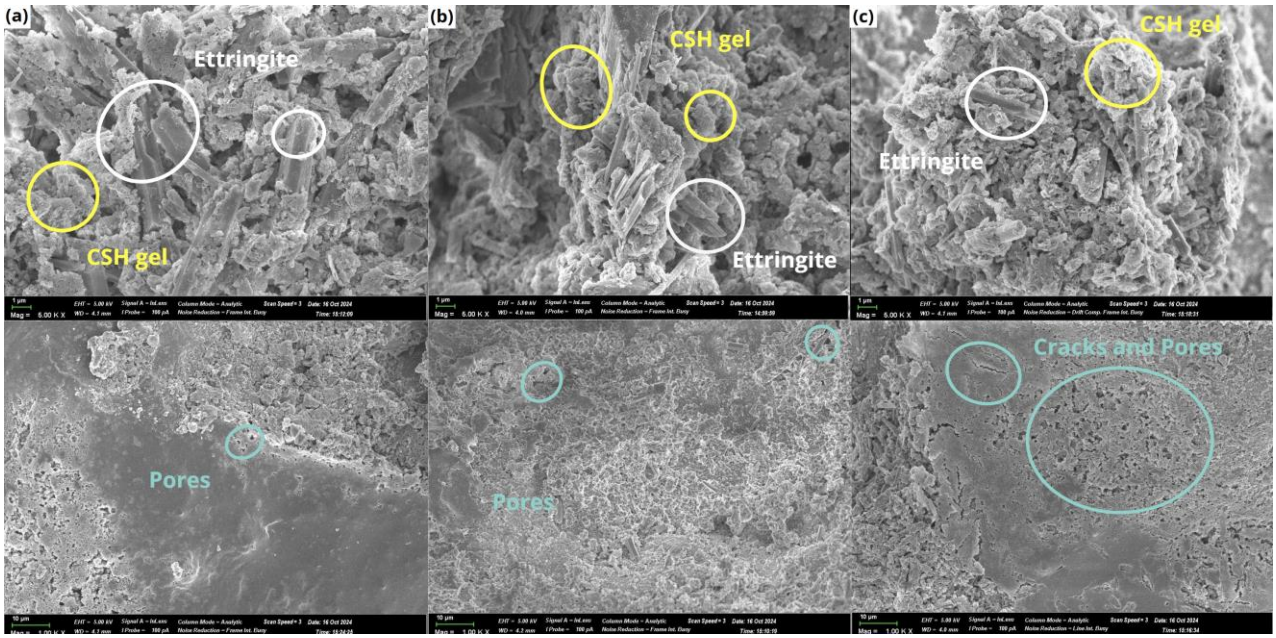

Fig. 11 Development of CSH gel and Ettringite at 7 curing days for different PG content: (a) 10%; (b) 30% and (c) 50%

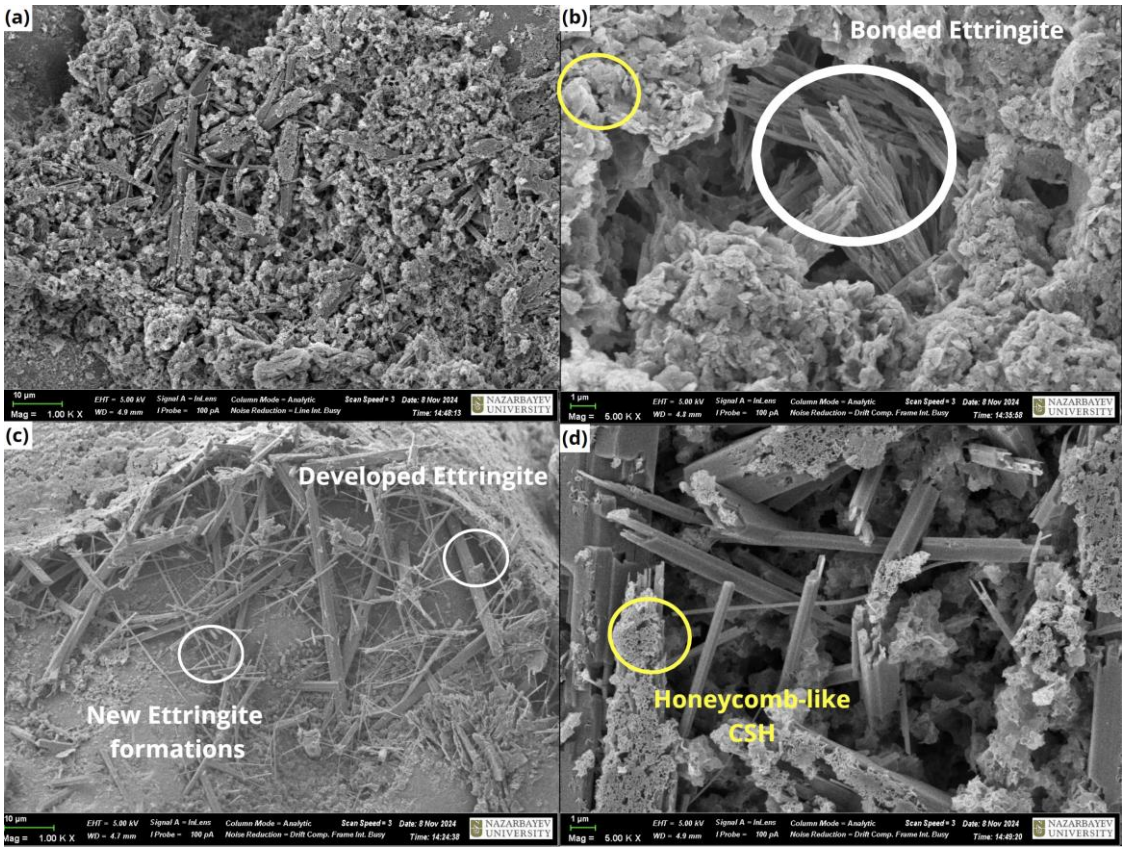

Fig. 12 Development of CSH gel and Ettringite at 28 curing days for 30% PG content (a) Densely packed, (b) Bonded ettringite, (c) Early and developed ettringite and (d) Honeycomb-like CSH

(Rauf *et al*. 2024, Sagidullina *et al*. 2023). The results from Rauf (2024) and Sagidullina (2023) align with those of this study, further reinforcing the role of PG replacement in influencing matrix densification, bond formation, and porosity characteristics in CSA-stabilized materials.

At 10% PG, acicular ettringite crystals is clearly visible, particularly in the lower part of the image. These needle-like structures contribute to strength development by binding particles and filling void spaces. The microstructure appears dense, with fewer visible pores, indicating improved material

compactness at this PG level.

At 30% PG replacement, the microstructure exhibits an increased presence of CSH gel and densely packed ettringite crystals, both of which are crucial for strength development. Minimal visible pores are present, suggesting a highly compact matrix. This concentration achieves the best balance between hydration product formation and material density, correlating with the highest UCS value observed in the study.

At 50% PG replacement, a reduction in CSH gel and ettringite formation is observed, accompanied by increased porosity and the presence of cracks. These features, highlighted in light blue, indicate that excessive PG content interferes with hydration reactions, reducing material strength and structural integrity.

Fig. 12 shows SEM images for the development of CSH gel and ettringite at 28 curing days for 30% PG replacement. Compared to the 7- day microstructure, the matrix displays a diverse range of features, including well-formed ettringite needles, CSH gel, honeycomb-like structures, and areas of densely bonded particles.

The densely packed structure in Fig. 12(a) demonstrates the cohesion achieved by the dispersed ettringite crystals and sand particles. In Fig. 12(b), bonded ettringite formations are clearly visible, with needle-like structures forming a cohesive network that strengthens the matrix. This dense arrangement fills void spaces and enhances durability. Fig. 12(c) highlights both developed and newly formed ettringite crystals, illustrating continuous hydration activity. The newly formed crystals fill remaining voids, maintaining material homogeneity and contributing to ongoing development of strength. Finally, Fig. 12(d) reveals a honeycomb-like CSH structure, which provides a stable framework for load distribution and enhances the durability of the composite. The interconnected network of CSH and ettringite phases reinforces the matrix, resulting in a material that resists external stresses effectively. These observations confirm that 30% PG replacement achieves the best microstructural properties, balancing hydration product formation, material density, and strength, making it the optimal PG content for soil stabilization.

4. Conclusions

The study investigated the microstructural and mechanical properties of CSA-treated sand with varying PG replacement concentrations, focusing on hydration product development, unconfined compressive strength (UCS) and ultrasonic pulse velocity (UPV). Based on the comprehensive analysis, the following conclusions were drawn:

1. The results demonstrate that 30% PG replacement provides an optimal balance between strength development and homogeneity. At this concentration, UCS reached its highest value, while UPV results confirmed improved compaction and reduced porosity over the curing period, as validated by SEM observations.
2. Microstructural analysis revealed that ettringite and CSH play complementary roles in improving material properties. Ettringite, with its needle-like structure, primarily facilitates early strength development by filling void spaces and linking particles. CSH, particularly in its honeycomb-like configuration, contributes to long-term material stability by forming a cohesive and durable matrix.
3. Longer curing times between 14 and 28 days, resulted in significant strength gains and improved homogeneity at all PG replacement levels. However, the 30% PG replacement consistently achieved superior strength and microstructural characteristics, indicating its suitability for optimal performance.
4. Different CSA concentrations (3%, 5%, and 7%) had a noticeable impact on UPV and UCS results. The combination of 7% CSA and 30% PG replacement exhibited the most consistent material properties. Higher CSA content accelerates hydration reactions, promoting the formation of ettringite and CSH phases, which enhanced material strength homogeneity.
5. The optimal 30% PG is a possible alternative to gypsum. UCS results with gypsum replacement were approximately 20% higher than those of phosphogypsum. This difference is attributed to the presence of impurities in raw PG, which may interfere with hydration reactions and strength development.

In summary, this study demonstrates that a 30% PG replacement with 7% CSA concentration provides a sustainable and efficient mix design for CSA-treated sand, achieving an optimal balance of strength, durability, and homogeneity. The findings confirm the feasibility of utilizing PG as a partial replacement material in construction applications, offering dual benefits: improved material performance and enhanced environmental sustainability by reducing industrial waste. Although the results highlight the potential of this approach, further long-term investigations are necessary to assess the evolution of strength development over time and the environmental implications of PG usage to ensure its safe and effective application in construction.

Acknowledgments

This research was funded by the Ministry of Education and Science (MES) Grant No. AP19675456, and Nazarbayev University, Collaborative Research Grant No. 111024CRP201. The authors extend their gratitude to “Kazphosphate” company in Taraz, Kazakhstan for providing the raw phosphogypsum materials used in this study. Their generous support is greatly appreciated. Any opinions, findings, conclusions, or recommendations expressed in this material are those of the author(s) and do not necessarily reflect the views of Nazarbayev University.

References

Akın Altun, İ. and Sert, Y. (2004), “Utilization of weathered phosphogypsum as set retarder in Portland cement”, *Cement Concrete Res.*, **34**(4), 677-680. https://doi.org/10.1016/j.cemconres.2003.10.017.

Ahmadullah, T. and Chrysochoou, M. (2024), “Relationship between strength development and pozzolanic reactions in lime stabilized kaolinite”, *Geo-Eng.*, **15**, 11.

https://doi.org/10.1186/s40703-024-00212-6.

Almeshal, I., Tayeh, B.A., Alyousef, R., Alabduljabbar, H. and Mohamed, A.M. (2020), "Eco-friendly concrete containing recycled plastic as partial replacement for sand", *J. Mater. Res. Tech.*, **9**(3), 4631-4643. https://doi.org/10.1016/j.jmrt.2020.02.090.

Aparna, R.P. and Bindu, J. (2023), "Utilization of waste materials as a substitute for the sand drain in clayey soil", *Int. J. Geo-Eng.*, **14**(1), N/A. https://doi.org/10.1186/s40703-022-00180-9

Cai, Q., Jiang, J., Ma, B., Shao, Z., Hu, Y., Qian, B. and Wang, L. (2021), "Efficient removal of phosphate impurities in waste phosphogypsum for the production of cement", *Sci. Total Environ*., **780**, 146600. https://doi.org/10.1016/j.scitotenv.2021.146600.

Chernysh, Y., Yakhnenko, O., Chubur, V. and Roubík, H. (2021), "Phosphogypsum recycling: A review of environmental issues, current trends, and prospects", *Appl. Sci*., **11**(4), 1575. https://doi.org/10.3390/app11041575.

Degirmenci, N., Okucu, A. and Turabi, A. (2007), "Application of phosphogypsum in soil stabilization", *Build. Environ.*, **42**(9), 3393-3398. https://doi.org/10.1016/j.buildenv.2006.08.010.

Gidebo, F.A., Yasuhara, H. and Kinoshita, N. (2023), "Stabilization of expansive soil with agricultural waste additives: A review", *Int. J. Geo-Eng*., **14**(1), 14. https://doi.org/10.1186/s40703-023-00194-x.

Guo, X., Shi, H., Hu, W. and Wu, K. (2014), "Durability and microstructure of CSA cement-based materials from MSWI fly ash", *Cement Concrete Compos*., **46**, 26-31. https://doi.org/10.1016/j.cemconcomp.2013.10.015.

Jain, A.K. (2024), "Exploring the viability of Bentonite-amended blends incorporating marble dust, sand, and fly ash for the creation of an environmentally sustainable landfill liner system", *Int. J. Geo-Eng*., **15**, 16. https://doi.org/10.1186/s40703-024-00214-4.

Jalili, J., Askari, F., Haghshenas, E. and Marghaiezadeh, A. (2023), "Investigation on economical method of foundation construction on soft soils in seismic zones: A case study in southern Iran", *Geomech. Eng*., **32**(2), 209-232. https://doi.org/10.12989/gae.2023.32.2.209.

Kayumov, A., Salimova, B., Khakimova, R. and Kayumov, A. (2021), "Strengthening the roadbed of highways using soil stabilizers", *E3S Web of Conferences*, **264**, 02012. https://doi.org/10.1051/e3sconf/202126402012.

Liu, D.S., Wang, C.Q., Mei, X.D. and Zhang, C. (2019), "An effective treatment method for phosphogypsum", *Environ. Sci. Pollut. R*., **26**(29), 30533-30539. https://doi.org/10.1007/s11356-019-06113-x

Liu, S., Wang, L. and Yu, B. (2019), "Effect of modified phosphogypsum on the hydration properties of the phosphogypsum-based supersulfated cement", *Constr. Build. Mater.,* **214**, 9-16. https://doi.org/10.1016/j.conbuildmat.2019.04.052.

Men, J., Li, Y., Cheng, P. and Zhang, Z. (2022), "Recycling phosphogypsum in road construction materials and associated environmental considerations: A review", *Heliyon*, **8**(11), e11518. https://doi.org/10.1016/j.heliyon.2022.e11518.

Meskini, S., Mechnou, I., Benmansour, M., Remmal, T. and Samdi, A. (2023), "Environmental investigation on the use of a phosphogypsum-based road material: Radiological and leaching assessment", *J. Environ. Management*, **345**, 118597. https://doi.org/10.1016/j.jenvman.2023.118597.

Murali, G. and Azab, M. (2023), "Recent research in utilization of phosphogypsum as building materials: Review", *J. Mater. Res. Tech*., **25**, 960-987. https://doi.org/10.1016/j.jmrt.2023.05.272.

Mustafayeva, A., Bimykova, A., Kim, J. and Moon, S.W. (2023a), "Soil stabilization with Basic Oxygen Furnace (BOF) slag", *In CRC Press*, 567-571. https://doi.org/10.1201/9781003299127-71.

Mustafayeva, A., Bimykova, A., Olagunju, S.O., Kim, J., Satyanaga, A. and Moon, S.W. (2023b), "Mechanical properties and microscopic mechanism of Basic Oxygen Furnace (BOF) slag-treated clay subgrades", *Buildings*, **13**(12), 2962. https://doi.org/10.3390/buildings13122962.

Ocheme, J.I., Kim, J. and Moon, S.W. (2024), "Enhancing geomechanical characteristics of calcium sulfoaluminate (CSA) cement-treated soil under low confining pressures", *Scientific Reports*, **14**(1), 11618. https://doi.org/10.1038/s41598-024-61548-8.

Ocheme, J.I., Olagunju, S.O., Khamitov, R., Satyanaga, A., Kim, J. and Moon, S.W. (2023), "Triaxial shear behavior of calcium sulfoaluminate (CSA)-treated sand under high confining pressures", *Geomech. Eng*., **33**(1), 41-51. https://doi.org/10.12989/gae.2023.33.1.041.

Park, S., Jeong, Y., Moon, J. and Lee, N. (2021), "Hydration characteristics of calcium sulfoaluminate (CSA) cement/portland cement blended pastes", *J. Build. Eng.*, **34**, 101880. https://doi.org/10.1016/j.jobe.2020.101880.

Qin, X., Cao, Y., Guan, H., Hu, Q., Liu, Z., Xu, J., Hu, B., Zhang, Z. and Luo, R. (2023), "Resource utilization and development of phosphogypsum-based materials in civil engineering", *J. Cleaner Product*., **387**, 135858. https://doi.org/10.1016/j.jclepro.2023.135858.

Rashad, A.M. (2017), "Phosphogypsum as a construction material", *J. Cleaner Product*., **166**, 732-743. https://doi.org/10.1016/j.jclepro.2017.08.049.

Rauf, A., Moon, S.W., Lim, C.K., Satyanaga, A. and Kim, J. (2024), "Mechanical characteristics of CSA-treated sand reinforced with fiber under freeze-thaw cycles", *Case Studies in Constr. Mater.*, **21**, e03875. https://doi.org/10.1016/j.cscm.2024.e03875

Regasa, H., Jothimani, M. and Oyda, Y. (2023), "Subgrade soil stabilization using the Quicklime: a case study from Modjo-Hawassa highway, Central Ethiopia", *Geo-Eng.*, **14**, 17. https://doi.org/10.1186/s40703-023-00197-8.

Saadaoui, E., Ghazel, N., Ben Romdhane, C. and Massoudi, N. (2017), "Phosphogypsum: Potential uses and problems – A review", *Int. J. Environ. Studies*, **74**(4), 558-567. https://doi.org/10.1080/00207233.2017.1330582.

Sagidullina, N., Abdialim, S., Kim, J., Satyanaga, A. and Moon, S.W. (2022a), "Influence of freeze–thaw cycles on physical and mechanical properties of cement-treated silty sand", *Sustainability,* **14**(12), 7000. https://doi.org/10.3390/su14127000.

Sagidullina, N., Muratova, A., Kim, J., Satyanaga, A. and Moon, S.W. (2023), "Stabilization of organic soil with CSA cement", *In CRC Press*, 578-582. https://doi.org/10.1201/9781003299127-73.

Sagidullina, N., Shynggys, S., Kim, J., Alfrendo, A. and Moon, S.W. (2022b), "Stabilization of silty sand with CSA cement under freeze-thaw cycles", *Proceedings of the 10th International Conference on Physical Modelling in Geotechnics (ICPMG).*

Subramanian, S., Khan, Q., Moon, S.W. and Ku, T. (2024), "A review of mix design terminologies for cement admixed sandy clay", *E3S Web of Conferences*, **544**, 11005. https://doi.org/10.1051/e3sconf/202454411005.

Subramanian, S., Moon, S.W. and Ku, T. (2019), "Effect of gypsum on the strength of CSA-treated sand", *Proceedings of the 16th Asian Regional Conference on Soil Mechanics and Geotechnical Engineering.*

Tao, Y., Rahul, A.V., Mohan, M.K., De Schutter, G. and Van Tittelboom, K. (2023), "Recent progress and technical challenges in using calcium sulfoaluminate (CSA) cement", *Cement Concrete Compos.,* **137**, 104908.

https://doi.org/10.1016/j.cemconcomp.2022.104908.
Vinoth, G., Moon, S., Moon, J. and Ku, T. (2018), "Early strength development in cement-treated sand using low-carbon rapid-hardening cements", *Soils Found.*, 58(5), 1200-1211. https://doi.org/10.1016/j.sandf.2018.07.001.
Wu, F., Chen, B., Qu, G., Liu, S., Zhao, C., Ren, Y. and Liu, X. (2022), "Harmless treatment technology of phosphogypsum: Directional stabilization of toxic and harmful substances", *J. Environ. Management*, **311**, 114827. https://doi.org/10.1016/j.jenvman.2022.114827.
Zivari, A., Siavoshnia, M. and Rezaei, H. (2023) "Effect of lime-rice husk ash on geotechnical properties of loess soil in Golestan province, Iran", *Geo-Eng.*, **14**, 20. https://doi.org/10.1186/s40703-023-00199-6.
Zheng, P., Li, W., Ma, Q. and Xi, L. (2023), "Mechanical properties of phosphogypsum-soil stabilized by lime activated ground granulated blast-furnace slag", *Constr. Build. Mater.*, **402**, 132994. https://doi.org/10.1016/j.conbuildmat.2023.132994.